

Molecular Dynamics and Experimental Study of Conformation Change of Poly(*N*-isopropylacrylamide) Hydrogels in Mixtures of Water and Methanol

Jonathan Walter,[†] Jan Sehart,[†] Jadran Vrabec,[‡] and Hans Hasse^{*,†}

[†]Laboratory of Engineering Thermodynamics, University of Kaiserslautern, Kaiserslautern, Germany

[‡]Thermodynamics and Energy Technology, University of Paderborn, Paderborn, Germany

S Supporting Information

ABSTRACT: The conformation transition of poly(*N*-isopropylacrylamide) hydrogel as a function of the methanol mole fraction in water/methanol mixtures is studied both experimentally and by atomistic molecular dynamics simulation with explicit solvents. The composition range in which the conformation transition of the hydrogel occurs is determined experimentally at 268.15, 298.15, and 313.15 K. In these experiments, cononsolvency, i.e., collapse at intermediate methanol concentrations while the hydrogel is swollen in both pure solvents, is observed at 268.15 and 298.15 K. The composition range in which cononsolvency is present does not significantly depend on the amount of cross-linker. The conformation transition of the hydrogel is caused by the conformation transition of the polymer chains of its backbone. Therefore, conformation changes of single backbone polymer chains are studied by massively parallel molecular dynamics simulations. The hydrogel backbone polymer is described with the force field OPLS-AA, water with the SPC/E model, and methanol with the model of the GROMOS-96 force field. During simulation, the mean radius of gyration of the polymer chains is monitored. The conformation of the polymer chains is studied at 268, 298, and 330 K as a function of the methanol mole fraction. Cononsolvency is observed at 268 and 298 K, which is in agreement with the present experiments. The structure of the solvent around the hydrogel backbone polymer is analyzed using H-bond statistics and visualization. It is found that cononsolvency is caused by the fact that the methanol molecules strongly attach to the hydrogel's backbone polymer, mainly with their hydroxyl group. This leads to the effect that the hydrophobic methyl groups of methanol are oriented toward the bulk solvent. The hydrogel+solvent shell hence appears hydrophobic and collapses in water-rich solvents. As more methanol is present in the solvent, the effect disappears again.



■ INTRODUCTION

Hydrogels are three-dimensional hydrophilic polymer networks. Their most characteristic property is their swelling in aqueous solutions. Hydrogels are used in many applications. Super absorbers, such as in diapers¹ and contact lenses,² are well established examples. Other interesting applications such as in drug delivery systems,³ tissue engineering,⁴ micro actuators,⁵ or epicardial restraint therapies,⁶ are discussed. To fully exploit the potential of hydrogels, it is crucial to understand, describe, and predict their swelling behavior.

The hydrogel that was studied in the present work is built up of poly(*N*-isopropylacrylamide) (PNIPAAm) and is cross-linked with *N,N*-methylenebisacrylamide (MBA). PNIPAAm is one of the most extensively studied hydrogels in the scientific literature and is mainly used in bioengineering applications.⁷ The degree of swelling of PNIPAAm in equilibrium is significantly influenced by the solvent type and the temperature.^{8–13} Upon variation of these factors, the hydrogel typically shows a region where it is swollen and a region where it is collapsed. In between those two regions lies the region of conformation transition.

Amiya et al.¹¹ measured the degree of swelling of PNIPAAm hydrogels as a function of the methanol mole fraction in

water/methanol mixtures at 273.15, 295.15, and 315.15 K. Mukae et al.¹² measured the same properties at 298.15 K, as well as Althans et al.¹⁴ at seven different temperatures between 298.15 and 308.15 K. These studies show that the hydrogel is collapsed above about 305 K in pure water and swollen in pure methanol. For all other studied temperatures, the hydrogel is swollen in both pure solvents, but shows a region in which it is collapsed at intermediate methanol concentrations. This phenomenon is termed cononsolvency.

For systems with PNIPAAm polymers, cononsolvency has been discussed in several studies.^{15–17} Winnik et al.¹⁷ investigated this phenomenon by means of the lower critical solution temperature (LCST) of the PNIPAAm polymer in water/methanol mixtures as a function of the methanol concentration.

The reasons for cononsolvency are discussed differently by different authors.^{12,15,17–19} In order to explain the different conformations of PNIPAAm in water/methanol mixtures, the behavior of the solvent molecules in the hydration shell of the

Received: December 22, 2011

Revised: March 17, 2012

Published: March 20, 2012

polymer or hydrogel was studied by monitoring the H-bonds or the interactions between the polymer and the two solvents with different experimental methods.

Mukea et al.¹² investigated PNIPAAm hydrogels in water/alcohol mixtures at 298.15 K. They measured the H-bonds between the hydrogel and the solvents with FTIR spectroscopy and found that the hydrogel is strongly dehydrated in the collapsed state. Therefore, the hydrogel mainly interacts with itself when collapsed. Further, they measured a higher amount of alcohol in the hydrogel than in the bulk solvent, leading to a higher degree of swelling in several pure alcohols than in pure water at 298.15 K. This leads to the conclusion that methanol is the better solvent. Mukea et al.¹² also found that the interactions between water and methanol are stronger than the ones between methanol and PNIPAAm when the hydrogel is collapsed. They compared the conformation transition with the partial molar volume of methanol in water/methanol mixtures, observing a minimum at approximately the same solvent composition and assumed a relation between these properties.

In contradiction to these results, Cheng et al.,¹⁹ using laser light scattering and FTIR, only found a weak decrease of the number of H-bonds when the polymer collapses in pure water above the LCST.

Winnik et al.¹⁷ investigated cononsolvency for PNIPAAm polymers in water/methanol mixtures at different temperatures. Using turbidity measurements, they found a flexible PNIPAAm coil in methanol and a stiffer and more elongated PNIPAAm coil in water. This led these authors to the conclusion that methanol is the better solvent for PNIPAAm.

Investigating the interactions between PNIPAAm polymers and the two solvent species in water/methanol mixtures, Schild et al.¹⁵ used infrared spectra, optical densities, and calorimetry. They came to the conclusion that the relevant interactions for the conformation transition are the ones between the polymer chain and the solvent molecules.

Tanaka et al.¹⁸ described the volume transition of PNIPAAm polymers in water/methanol mixtures based on models for cooperative and competitive hydration. They predicted a strong decrease of the H-bonds between the polymer and the solvents in the cononsolvency region and also stated that methanol is a better solvent for PNIPAAm than water.

Molecular dynamics simulations can give detailed insight into these phenomena on the atomistic level. The orientation of the solvents at the surface of PNIPAAm monomers in water/methanol mixtures was investigated in detail by Pang et al.²⁰ They found that the solvents are bound with their polar sites to the polar sites of the monomer.

In a preceding study of our group,²¹ it was shown that the conformation transition of PNIPAAm upon changing the temperature can be predicted by molecular simulation. In the present work, the influence of the solvent composition on the conformation transition of PNIPAAm in water/methanol mixtures was investigated. The effect was studied both by atomistic molecular dynamics simulation and by experiment. The molecular simulations were based on the force field OPLS-AA^{22,23} for PNIPAAm, SPC/E²⁴ for water, and different explicit models from the literature for methanol. The conformation transition of the hydrogel is dominated by the interactions between the solvent molecules and the hydrogel backbone polymer.²¹ Therefore, single PNIPAAm chains were investigated by molecular simulations. In these simulations, the radius of gyration and the structure of the solvent around single chains was monitored. The results were compared to the experimental

data for the degree of swelling of PNIPAAm hydrogel in water/methanol mixtures as a function of the methanol mole fraction at different temperatures.

■ EXPERIMENTAL PROCEDURE AND RESULTS

Chemically cross-linked hydrogels were synthesized in the present work by polymerizing *N*-isopropylacrylamide (NIPAAm) and by cross-linking it with MBA. The experimental method is only briefly described here, as it is the same as that described earlier by Hütther and Maurer.⁹ Polymerization and cross-linking were simultaneously carried out by free radical polymerization in oxygen-free deionized water at 298.15 K under nitrogen atmosphere. The reactions were initiated by small amounts of ammonium peroxodisulfate (starter) and sodium disulfite (accelerator).

For the synthesis, the monomer NIPAAm (Aldrich, 97%, CAS 2210-25-5), the cross-linking agent MBA (Fluka, ≥ 99%, CAS 110-26-9), and the initiators ammonium peroxodisulfate ((NH₄)₂S₂O₈) (Aldrich, ≥ 98%, CAS 7727-54-0) and sodium disulfite (Na₂S₂O₅) (Fluka, ≥ 98%, CAS 7681-57-4) were used without further purification. Oxygen-free, bidistilled water was used for synthesis. After synthesis, the hydrogel particles were thoroughly washed with deionized water and dried in a vacuum oven.

Hydrogels can not be characterized by a few numbers like it is done with specification chemicals. They are rather characterized by their production process. The following concentrations refer to the aqueous solution in which the polymerization was carried out: total mass fraction x_{gel}^m of polymerizable material

$$x_{\text{gel}}^m = \frac{m_{\text{NIPAAm}} + m_{\text{MBA}}}{m_{\text{total}}} \quad (1)$$

mole fraction of cross-linking agent x_{MBA}^n

$$x_{\text{MBA}}^n = \frac{n_{\text{MBA}}}{n_{\text{NIPAAm}} + n_{\text{MBA}}} \quad (2)$$

and mass fraction of the initiator x_s^m

$$x_s^m = \frac{m_s}{m_{\text{total}}} \quad (3)$$

Here, m and n are the mass and mole number, respectively. The parameters for the two hydrogels synthesized in the present work are presented in Table 1. The hydrogels differ mainly in the degree of cross-linking.

Table 1. Characterization of the Present Hydrogel Synthesis^a

hydrogel	$x_{\text{gel}}^m/\text{g}\cdot\text{g}^{-1}$	$x_{\text{MBA}}^n/\text{mol}\cdot\text{mol}^{-1}$	$x_s^m/\text{g}\cdot\text{g}^{-1}$
1	0.0800	0.02	4.244×10^{-4}
2	0.0797	0.01	4.186×10^{-4}

^aTotal mass fraction x_{gel}^m of polymerizable material, mole fraction of cross-linking agent x_{MBA}^n , and mass fraction of the initiator x_s^m . The two hydrogels differ mainly in the degree of cross-linking.

For each swelling experiment, 10 dried hydrogel particles were used. The amount of mass of the dried hydrogel particle was determined with a precision microbalance (type MX5, Mettler Toledo, Giessen, Germany) before the mixture of oxygen-free deionized water and methanol (Roth, 99%, CAS

67-56-1) was added to the particles. The solvent mixture was prepared with a precision balance (type XS4002S DeltaRange, Mettler Toledo, Gießen, Germany). The hydrogel in the solvent was then thermostatted for about 2 weeks. An air oven (type ICP 600, Memmert, Schwabach, Germany) was used at 298.15 and 313.15 K, a cryostat (type F34, Julabo, Seelbach, Germany) with a glycantine/water mixture as coolant was used at 268.15 K. For the temperature measurement, a calibrated platinum resistance thermometer with an overall uncertainty of ± 0.1 K was used. After reaching equilibrium, the hydrogel particles were taken out of the solvent, and the surface solvent was removed. The mass of the swollen particles was then determined with the precision microbalance. The degree of swelling of each particle was calculated as the ratio of mass of the swollen hydrogel m_{gel} to the mass of the dry hydrogel $m_{\text{gel}}^{\text{dry}}$

$$q = \frac{m_{\text{gel}}}{m_{\text{gel}}^{\text{dry}}} \quad (4)$$

For the 10 particles, the arithmetic mean and the standard deviation of the degree of swelling were calculated. The experiments were performed at temperatures of 268.15, 298.15, and 313.15 K for various compositions of the water/methanol mixture. The experimental results are summarized in Tables 2 and 3.

Table 2. Degree of Swelling q of Hydrogel 1 ($x_{\text{MBA}}^m = 0.02 \text{ g} \cdot \text{g}^{-1}$) in Water/Methanol Mixtures as a Function of the Mole Fraction of Methanol x_{MeOH}^n at Three Temperatures^a

$x_{\text{MeOH}}^n / \text{mol} \cdot \text{mol}^{-1}$	$q / \text{g} \cdot \text{g}^{-1}$		
	268.15 K	298.15 K	313.15 K
0.000	—	24.04 ± 0.56	1.77 ± 0.08
0.100	34.52 ± 2.02	11.44 ± 0.65	1.70 ± 0.04
0.200	23.70 ± 1.45	1.93 ± 0.04	2.04 ± 0.09
0.300	9.15 ± 0.24	2.37 ± 0.03	2.31 ± 0.04
0.400	9.72 ± 0.41	4.35 ± 0.15	3.56 ± 0.06
0.500	14.97 ± 0.88	11.63 ± 0.61	12.56 ± 0.55
0.601	18.92 ± 0.36	16.69 ± 0.21	17.19 ± 0.39
0.700	20.91 ± 0.41	19.69 ± 0.35	19.38 ± 0.22
0.800	22.35 ± 0.39	21.05 ± 0.29	20.61 ± 0.26
0.902	22.34 ± 0.73	21.34 ± 0.24	20.65 ± 0.70
1.000	21.96 ± 0.65	20.76 ± 0.53	19.91 ± 0.23

^aThe numbers behind \pm denote the standard deviation.

Table 3. Degree of Swelling q of Hydrogel 2 ($x_{\text{MBA}}^m = 0.01 \text{ g} \cdot \text{g}^{-1}$) in Water/Methanol Mixtures as a Function of the Mole Fraction of Methanol x_{MeOH}^n at Three Temperatures^a

$x_{\text{MeOH}}^n / \text{mol} \cdot \text{mol}^{-1}$	$q / \text{g} \cdot \text{g}^{-1}$		
	268.15 K	298.15 K	313.15 K
0.000	—	34.02 ± 1.28	1.54 ± 0.05
0.100	58.73 ± 1.55	1.91 ± 0.06	1.58 ± 0.06
0.200	50.43 ± 1.81	2.10 ± 0.04	1.78 ± 0.04
0.300	7.41 ± 0.60	2.58 ± 0.11	2.21 ± 0.02
0.400	9.02 ± 0.75	5.24 ± 0.31	4.72 ± 0.06
0.500	20.52 ± 0.51	17.81 ± 0.67	16.68 ± 0.52
0.601	26.09 ± 0.56	24.76 ± 0.62	23.35 ± 0.65
0.700	29.10 ± 1.29	27.00 ± 1.60	27.67 ± 0.34
0.800	30.43 ± 1.24	29.04 ± 0.88	29.16 ± 0.59
0.902	30.76 ± 1.25	30.59 ± 0.48	29.88 ± 0.51
1.000	30.75 ± 1.02	29.01 ± 1.02	28.69 ± 0.48

^aThe numbers behind \pm denote the standard deviation.

DISCUSSION OF EXPERIMENTAL RESULTS

Figures 1 and 2 present experimental results for the degree of swelling of the two hydrogels in water/methanol mixtures for

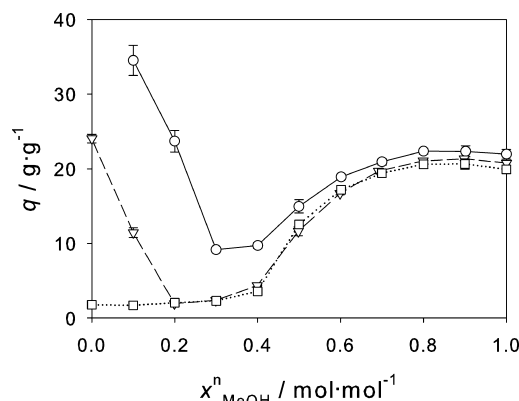


Figure 1. Degree of swelling q of the PNIPAAm Hydrogel 1 ($x_{\text{MBA}}^m = 0.02 \text{ mol} \cdot \text{mol}^{-1}$) in water/methanol mixtures at 268.15 K (\circ), 298.15 K (∇), and 313.15 K (\square) as a function of the mole fraction of methanol x_{MeOH}^n . Symbols: experimental data from this work; lines: guide for the eye. The error bars denote the standard deviation.

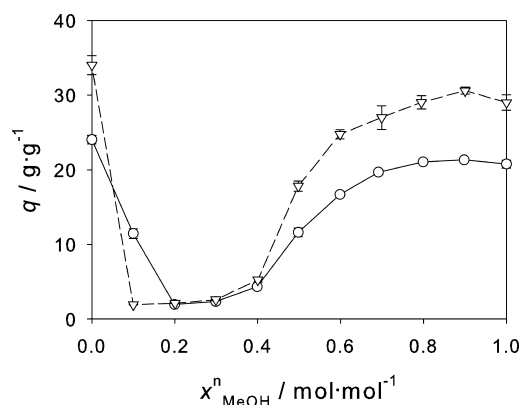


Figure 2. Degree of swelling q of the PNIPAAm Hydrogel 1 ($x_{\text{MBA}}^m = 0.02 \text{ mol} \cdot \text{mol}^{-1}$) (\circ) and Hydrogel 2 ($x_{\text{MBA}}^m = 0.01 \text{ mol} \cdot \text{mol}^{-1}$) (∇) in water/methanol mixtures as a function of the mole fraction of methanol x_{MeOH}^n at 298.15 K. Symbols: experimental data from this work; lines: guide for the eye. The error bars denote the standard deviation.

different temperatures as a function of the mole fraction of methanol. Figure 1 shows the influence of the temperature on the degree of swelling of Hydrogel 1. The influence of the amount of cross-linker is discussed by directly comparing the results for Hydrogel 1 and Hydrogel 2 at 298.15 K in Figure 2. The error bars denote the standard deviation, which is mostly within symbol size.

The results for Hydrogel 1 are presented in Figure 1. For all three temperatures, the hydrogel is swollen in pure methanol. The degree of swelling in pure methanol and methanol-rich mixtures is only very weakly temperature dependent. Higher temperatures lead to a lower degree of swelling. In pure water, the hydrogel is swollen at 298.15 K and collapsed at 313.15 K. At 298.15 K, the hydrogel shows a stronger swelling in pure water than in pure methanol. At 268.15 K, the degree of swelling can not be measured in pure water, because it is below freezing temperature. At 268.15 and 298.15 K, cononsolvency was observed: even though the hydrogel is swollen in both pure water (or water-rich mixtures at 268.15 K) and pure methanol,

there is a composition range of the solvent mixture where the hydrogel is collapsed. Adding small amounts of methanol to pure water leads to a strong decrease of the degree of swelling, whereas adding small amounts of water to pure methanol has hardly any effect. There seems to be a shallow local maximum of the degree of swelling in the region of high methanol mole fractions. Thus, the cononsolvency region is observed on the water-rich side of the diagram shown in Figure 1. In the cononsolvency region at 298.15 K, the hydrogel collapses significantly, but not to the level that is observed at the other temperatures. This is supported by the findings of Winnik et al.,¹⁷ who reported no cononsolvency for PNIPAAm polymers in water/methanol mixtures below about 263 K.

For Hydrogel 2, the results are qualitatively the same as those for Hydrogel 1. These results are presented in Table 3. In Figure 2, the two hydrogels are compared for the temperature of 298.15 K. The two hydrogels mainly differ in the degree of cross-linking (cf. Table 1). The degree of swelling is higher for Hydrogel 1, which has a lower degree of cross-linking. The solvent composition range, in which cononsolvency was observed is hardly influenced by the degree of cross-linking. This corroborates that cononsolvency is caused by the interactions between the hydrogel backbone polymer and the solvent molecules. This is in line with the finding that the volume transition of hydrogels upon temperature change also does not significantly depend on the degree of cross-linking.²¹

The results of the swelling experiments of PNIPAAm hydrogels can be compared with the solubility experiments of PNIPAAm polymers in water/methanol mixtures by Winnik et al.,¹⁷ where cloud points were measured. The volume transition of hydrogels and the solubility of the backbone polymer are closely related properties, as both depend on the interactions between the polymer and the solvent. A direct quantitative comparison, however, is not straightforward, especially as the volume transition of the hydrogel does not take place at a specific composition, but rather over a composition range that may be wide. In the present work, an empirical approach was followed to achieve a mapping. The crucial step in that approach is to determine a certain solvent composition at which the volume transition occurs (transition point) from the hydrogel swelling data. In reality, there is rather a composition range, such that a specific methanol mole fraction has to be chosen suitably by a well-defined procedure which will, however, unavoidably be somewhat arbitrary.

For the definition of that "transition point", in the present work, the degree of swelling q^* at that point was specified and then the composition $x_{\text{MeOH}}^{\text{tr}}$ of the transition point was determined from the plot of $q(x_{\text{MeOH}})$ (cf. Figures 1 and 2). For that definition of q^* , the minimum of q observed at 268.15 K was selected (Hydrogel 1: $8.5 \text{ g} \cdot \text{g}^{-1}$, Hydrogel 2: $9.5 \text{ g} \cdot \text{g}^{-1}$). The temperature of 268.15 K is close to the lowest temperature of the cloud point curve observed by Winnik et al.¹⁷ so that no full collapse was observed. Note also that q^* for Hydrogel 1 corresponds to a transition temperature $T^* = 305 \text{ K}$ in plots of $q(T)$ for that hydrogel,²¹ which is in good agreement with other data that are reported for that transition in the literature.^{25,26}

The results for the transition mole fraction $x_{\text{MeOH}}^{\text{tr}}$ for different temperatures are listed in Table 4 and shown in Figure 3, where they are compared with the experimental results of Winnik et al.¹⁷ In Figure 3, the cloud point curve of the polymer is compared to the data estimated from the hydrogel volume transition, showing the relation between the temperature and the solvent composition at the transition points.

Table 4. Transition Points $x_{\text{MeOH}}^{\text{tr}}$ for Hydrogel 1 ($x_{\text{MBA}}^{\text{tr}} = 0.02 \text{ g} \cdot \text{g}^{-1}$) and Hydrogel 2 ($x_{\text{MBA}}^{\text{tr}} = 0.01 \text{ g} \cdot \text{g}^{-1}$) as Estimated with the Empirical Procedure Described in the Text: Relation between Temperature and Methanol Mole Fraction^a

hydrogel	$x_{\text{MeOH}}^{\text{tr}} / \text{mol} \cdot \text{mol}^{-1}$		
	268.15 K	298.15 K	313.15 K
1	0.30/0.38	0.08/0.43	0.43
2	0.30/0.40	0.12/0.47	0.47

^aIf two values are listed, cononsolvency was observed. Starting from small methanol mole fractions, the lower number corresponds to the collapse, the higher number to the re-swelling.

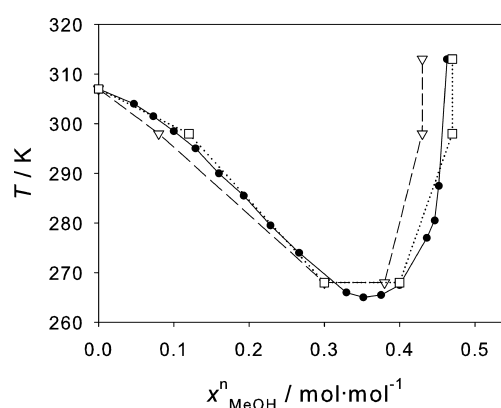


Figure 3. Comparison of transition points of PNIPAAm in water/methanol mixtures determined in different ways: Estimates from the present experimental results for PNIPAAm Hydrogel 1 ($x_{\text{MBA}}^{\text{tr}} = 0.02 \text{ g} \cdot \text{g}^{-1}$) (\square) and Hydrogel 2 ($x_{\text{MBA}}^{\text{tr}} = 0.01 \text{ g} \cdot \text{g}^{-1}$) (∇) as well as experimental cloud point data for PNIPAAm polymers by Winnik et al.¹⁷ (\bullet).

The comparison shows that the conditions for which the volume transition of the PNIPAAm hydrogel was observed and the cloud point of the PNIPAAm polymer are almost identical. Furthermore, it was found that the effect does not significantly depend on the amount of cross-linker. Both findings support the interpretation that the volume transition of the hydrogel is an effect related to the interactions between backbone polymer and solvent molecules.

■ FORCE FIELDS

For the present molecular dynamics simulations of PNIPAAm in water/methanol mixtures, the OPLS-AA (OPLS) force field^{22,23} was used to describe PNIPAAm. It was combined with the SPC/E water model.²⁴ In a preceding study,²¹ it was shown that this combination is suited for predicting the conformation change of PNIPAAm in water as a function of the temperature. The Lennard-Jones (LJ) and point charge parameters of the OPLS force field used for PNIPAAm are given in Table 5.

For methanol, the model of GROMOS96 with low point charges (G96-low)²⁷ was used. The potential and geometry parameters are listed in Tables 6 and 7, respectively. Two other methanol models (Schnabel et al.²⁸ and GROMOS96 with high point charges²⁷) were also tested in preliminary studies, but were not found to yield cononsolvency. The results of these preliminary studies are briefly presented in Appendix A in the Supporting Information.

Table 5. LJ Parameters σ and ϵ and Point Charge Magnitude q_{el} of the PNIPAAm Force Field OPLS,^{22,23} where e is the Elementary Charge

site	σ/nm	$\epsilon/\text{kJ}\cdot\text{mol}^{-1}$	q_{el}/e
C	0.375	0.4393	0.50
O	0.296	0.8786	-0.50
N	0.325	0.7113	-0.50
H	—	—	0.30
CH(-N)	0.350	0.2761	0.14
CH	0.350	0.2761	-0.06
CH ₂	0.350	0.2761	-0.12
CH ₃	0.350	0.2761	-0.18
H in CH _x	—	—	0.06

Table 6. LJ Parameters σ and ϵ and Point Charge Magnitude q_{el} of the Methanol Model G96-low,²⁷ where e is the Elementary Charge

site	σ/nm	$\epsilon/\text{kJ}\cdot\text{mol}^{-1}$	q_{el}/e
CH ₃	0.3552	1.1038	0.290
O	0.3143	0.6785	-0.690
H	—	—	0.400

Table 7. Bond Lengths r , Bond Angles α , and Force Constants k of the Harmonic Potentials of the Methanol Model G96-low²⁷

$r_{\text{C-O}}$ nm	$k_{\text{b,C-O}}$ $\text{kJ}\cdot\text{mol}^{-1}\text{nm}^{-2}$	$r_{\text{O-H}}$ nm	$k_{\text{b,O-H}}$ $\text{kJ}\cdot\text{mol}^{-1}\text{nm}^{-2}$	$\alpha_{\text{C-O-H}}$	$k_{\alpha,\text{C-O-H}}$ $\text{kJ}\cdot\text{mol}^{-1}\text{rad}^{-2}$
0.136	376560	0.100	313800	108.53°	397.5

For the unlike LJ pair interaction, a geometric mean mixing rule for both σ and ϵ was used, as specified by the OPLS force field

$$\begin{aligned}\sigma_{ij} &= \sqrt{\sigma_i \cdot \sigma_j} \\ \epsilon_{ij} &= \sqrt{\epsilon_i \cdot \epsilon_j}\end{aligned}\quad (5)$$

For the intramolecular interactions, the method of the 1–4 interactions was employed.²⁹ Thereby, the interactions between a given atom and its first and second neighbors were only modeled by the bond and the angle term. Interactions between the atom and its third neighbor were calculated by the dihedral, the Coulomb interaction, and the LJ term. The last two terms were reduced by a scaling factor of 0.5. All other intramolecular interactions were modeled with the unmodified Coulomb interaction and the LJ term.

SIMULATION METHODS

Molecular simulations of PNIPAAm single chains were carried out with version 4.0.5 of the GROMACS simulation package,^{30,31} which was developed for the simulation of large molecules in solutions.

Single PNIPAAm chains in water were simulated in the isothermal–isobaric ensemble. The pressure was specified to be 1 bar and was controlled by the Berendsen barostat,³² the temperature was controlled by the velocity-rescale thermostat,³³ and the time step was 1 fs for all simulations. The standard deviation of the temperature over time was about 1.3 K.²¹ Newton's equations of motion were numerically solved with the leapfrog integrator.³⁴ The cutoff radius was $r_c = 1.5$ nm

for all interactions. For the long-range electrostatic interactions, particle mesh Ewald³⁵ with a grid spacing of 0.12 nm and an interpolation order of 4 was used.

The simulations were carried out with PNIPAAm chains of 30 monomers as in ref 21. For setting up the starting conformation, the procedure suggested in ref 21 was adopted. A stretched configuration derived from a simulation of the polymer chain in pure water in equilibrium at 280 K was used. Prior to the simulations, the solvent mixtures were equilibrated using about 3500 solvent molecules over 2×10^6 time steps monitoring the density. The equilibrated solvent was then used to solvate the PNIPAAm chain. The simulation volume was about $14 \times 6 \times 6$ nm and contained in addition to the single PNIPAAm chain about 14000 solvent molecules. After solvent equilibration over $1-5 \times 10^6$ timesteps with a fixed polymer configuration and production runs over $2-8 \times 10^7$ time steps (20–80 ns) were carried out.

In order to analyze the results, the radius of gyration R_g was calculated

$$R_g = \left(\frac{\sum_i \|r_i\|^2 m_i}{\sum_i m_i} \right)^{1/2} \quad (6)$$

which characterizes the degree of stretching of the chain, where m_i is the mass of site i and $\|r_i\|$ is the norm of the vector from site i to the center of mass of the chain. The radius of gyration in equilibrium was calculated as the arithmetic mean over the last 10^7 time steps of the run (1000 samples) together with its standard deviation.

In order to investigate the structure of the solvent species around the PNIPAAm chain, the average number of H-bonds between the polar amide group of the chain and the solvent molecules was measured. For identifying H-bonds, a geometric criterion was employed, which is based on the distance between acceptor and donor and the angle acceptor–donor–hydrogen. A H-bond was assumed to be present if the distance was below 0.3 nm and the angle smaller than 30°.^{36,37}

For further information about the structure of the solvent around the PNIPAAm chains, in some simulations, the backbone of the single chain was visualized together with the solvent molecules of the hydration shell using VMD³⁸ and MegaMol.^{39,40}

The simulations were performed on the high-performance computer HP XC 4000 at the Steinbuch Centre for Computing in Karlsruhe (Germany), which is equipped with Opteron 2.6 GHz Dual Core processors. In typical runs, 128 cores were used. Preliminary studies of strong scaling of GROMACS on that hardware show that the program can be used efficiently up to about that number of processors.⁴¹ Typical runs consumed about 18000 CPU h.

SIMULATION RESULTS

Simulations of PNIPAAm chains of 30 monomers in water/methanol mixtures of different compositions were carried out at 268, 298, and 330 K to determine the radius of gyration of the polymer in equilibrium. The simulation results are summarized in Table 8 and presented graphically in Figure 4, which shows the radius of gyration in equilibrium as a function of the mole fraction of methanol.

The results at 268 K are presented in the top panel of Figure 4. In pure methanol and in water-rich mixtures, the single chain is stretched. There is no data for pure water because it is

Table 8. Radius of Gyration R_g of a PNIPAAm Chain of 30 Monomers in Water/Methanol Mixtures in Equilibrium as a Function of the Methanol Mole Fraction x_{MeOH}^n at Three Different Temperatures^a

$x_{\text{MeOH}}^n / \text{mol} \cdot \text{mol}^{-1}$	R_g / nm		
	268 K	298 K	330 K
0.000	—	1.92 ± 0.05	1.11 ± 0.03
0.110	—	1.11 ± 0.04	—
0.202	1.73 ± 0.05	1.05 ± 0.05	1.19 ± 0.07
0.297	—	1.59 ± 0.12	—
0.411	1.58 ± 0.12	1.74 ± 0.07	1.27 ± 0.09
0.487	1.84 ± 0.06	—	1.45 ± 0.17
0.579	1.23 ± 0.07	1.79 ± 0.08	1.68 ± 0.08
0.692	1.71 ± 0.11	—	—
0.790	1.79 ± 0.06	1.70 ± 0.01	1.63 ± 0.10
1.000	1.66 ± 0.09	1.76 ± 0.08	1.46 ± 0.13

^aThe numbers behind \pm denote the standard deviation.

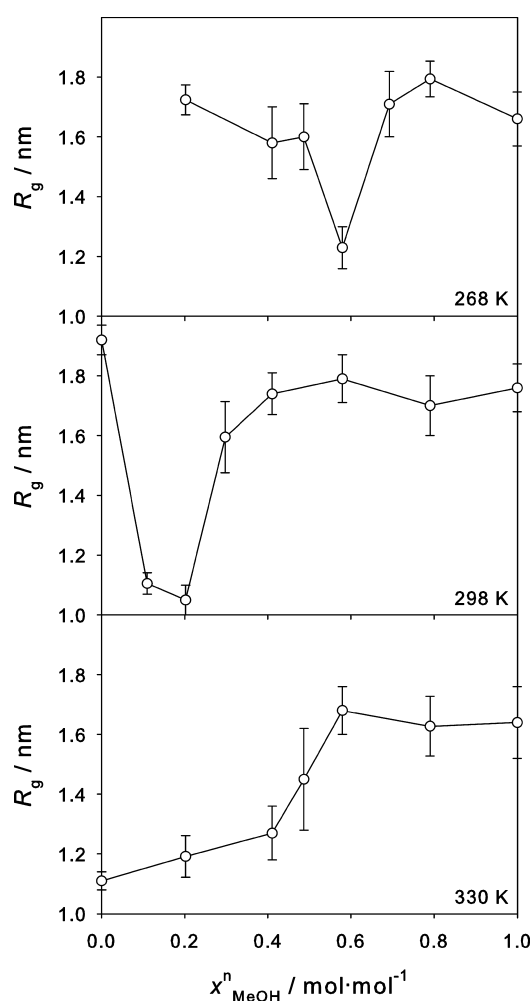


Figure 4. Radius of gyration R_g of a PNIPAAm chain of 30 monomers in water/methanol mixtures in equilibrium as a function of the methanol mole fraction x_{MeOH}^n at 268, 298, and 330 K. The error bars indicate the standard deviation. There are no results for pure water at 268 K, because it is solid at this temperature.

solid at this temperature. The results show a small region of cononsolvency at methanol mole fractions of about $0.6 \text{ mol} \cdot \text{mol}^{-1}$. The observation of cononsolvency at this temperature is in agreement with the experimental data, even though the

composition range in which cononsolvency occurs is not correctly predicted. The experiments from the present work on PNIPAAm hydrogels as well as the experimental results on PNIPAAm polymers of Winnik et al.¹⁷ indicate that cononsolvency does not exist at temperatures substantially below 268 K. The simulation result with the small cononsolvency region at 268 K is in line with these observations.

The central panel of Figure 4 shows the results at 298 K. Again, in both pure solvents, the single chain is stretched, for intermediate methanol mole fractions between 0.1 and $0.2 \text{ mol} \cdot \text{mol}^{-1}$, it is collapsed. The region of cononsolvency is predicted to be much larger than at 268 K and is now in the composition range in which it was also observed experimentally (cf. Figure 1).

The results at 330 K are presented in the bottom panel of Figure 4. In pure water, the single chain is collapsed, in pure methanol, it is stretched. In the mixture, at methanol mole fractions above about $0.6 \text{ mol} \cdot \text{mol}^{-1}$, the chain is stretched. This is in fair agreement with the results obtained with the present experiments at the highest studied temperature of 313 K (cf. Figure 1). These temperatures are compared with each other because they are both somewhat above the transition temperature in pure water, which is about 305 K as determined by experiment and about 320 K as determined by molecular simulation.²¹

These results show that it is possible to qualitatively predict the volume transition of hydrogels by molecular simulation if suitable force fields are chosen. This is encouraging, as the underlying force fields were developed using only information that is unrelated to the phenomenon studied here, and no further adjustments were made.

However, molecular simulation offers more than just the possibility to predict the volume transition. The extremely highly resolved information provided by such simulations allows gaining insight into the reasons for cononsolvency. For that purpose, the structure of the solvent around the PNIPAAm chain was studied both by H-bond statistics and visualization.

The number of H-bonds between the two solvent species and the amide groups of the PNIPAAm chain was determined for the equilibrated chain. The H-bonds form between the oxygen atom of the amide group and the hydrogen atoms of the solvents as well as between the hydrogen atom of the amide group and the oxygen atoms of the solvents (cf. Appendix B in the Supporting Information). In principle, the nitrogen atom of the amide group of PNIPAAm may also act as a H-bond acceptor. The results obtained in the present study show that the number of H-bonds that involve this nitrogen atom is so small that it can be neglected. They also show that the amount of intramolecular H-bonding of the PNIPAAm chain is small compared to the number of intermolecular H-bonds between the chain and the solvent molecules. Thus intramolecular H-bonding is neglected in the following. The low number of intramolecular H-bonds may be due to the chain length chosen in the present study, but the same results were also found for longer chains and three-dimensional networks that were also simulated here.

Figure 5 shows the average number of H-bonds between a monomer unit of the PNIPAAm chain and water or methanol, respectively, as a function of the methanol mole fraction at 298 K. For comparison, the radius of gyration of the single chain is plotted as well. Furthermore, Figure 5 contains linear interpolations between the number of H-bonds in the two pure solvents and zero for the case in which the solvent is not present. It can be seen that less H-bonds are present in pure

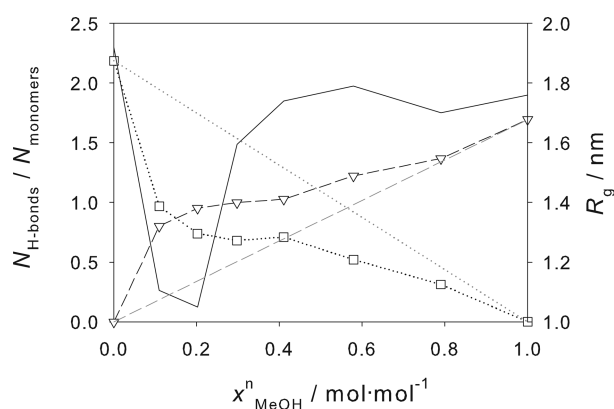


Figure 5. Average number of H-bonds between methanol (∇) or water (\square) and a monomer unit of the PNIPAAm chain as a function of the methanol mole fraction x_{MeOH}^n at 298 K and 1 bar. Additionally, the radius of gyration R_g (—) is shown as well as linear interpolations between the number of H-bonds for the pure solvents methanol (---) or water (···) and zero where the solvent is not present in the mixture.

methanol than in pure water, which is related to the stronger stretching of the chain in water than in methanol. However, despite this, in mixtures of these solvents, the PNIPAAm chain has a stronger preference for forming H-bonds with methanol than with water. Considering the entire composition range from pure water to pure methanol, the number of H-bonds with methanol increases more than the linear interpolation while the number of H-bonds with water decreases more than the linear interpolation. Thus, the number of H-bonds of the PNIPAAm chain with methanol exceeds the number of H-bonds with water already at methanol mole fractions of about $0.15 \text{ mol}\cdot\text{mol}^{-1}$. The occurrence of cononsolvency upon increasing the methanol mole fraction goes along with a strong decrease of the number of H-bonds between water and the PNIPAAm chain and a strong increase of the corresponding H-bonds with methanol.

These results confirm that methanol is a better solvent for PNIPAAm than water. The PNIPAAm chain is collapsed in the region where the methanol concentration around PNIPAAm strongly differs from that in the bulk solvent. This indicates that the collapse of the polymer or hydrogel is related to interactions between the solvation shell around PNIPAAm and the rest of the solvent. This finding is in agreement with the conclusions Schild et al.¹⁵ based on their experimental studies of PNIPAAm polymers and hydrogels.

In Table 9, the average number of H-bonds between the two solvent species and the oxygen or the hydrogen atom of the

Table 9. Average Number of H-Bonds between Methanol or Water and the Oxygen or Hydrogen Atom of the Amide Group of a Monomer Unit of the PNIPAAm Chain for a Solvent Methanol Mole Fraction of $0.1 \text{ mol}\cdot\text{mol}^{-1}$ at 298 K

PNIPAAm	methanol	water
O	0.41	0.75
H	0.39	0.22

amide group of PNIPAAm are presented for a methanol mole fraction in the solvent of $0.1 \text{ mol}\cdot\text{mol}^{-1}$, which is inside the cononsolvency region. From these results, it can be seen that water is preferably attached to the oxygen atom and methanol to the hydrogen atom of the amide group. The hydrogen atom

is further away from the backbone of the PNIPAAm chain than the oxygen atom (cf. Figure 6). Therefore, water within the

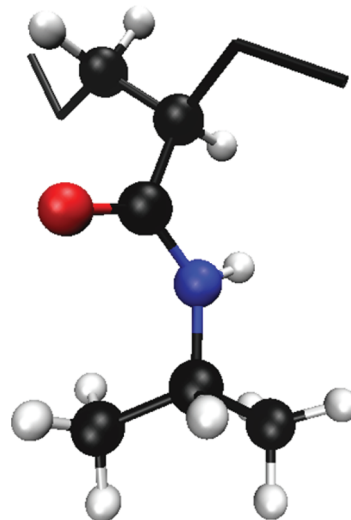


Figure 6. Snapshot of a PNIPAAm monomer from simulation. The colors indicate atom types: carbon (black), hydrogen (white), oxygen (red), and nitrogen (blue). The upper two carbon atoms are part of the polymer backbone, denoted by the black tubes. The lower three carbon atoms are the nonpolar end of the side group. In between these two sites are the four atoms of the polar amide group, which forms H-bonds with the solvent molecules.

solvation shell is preferably closer to the backbone, while methanol resides preferably in the outer regions of the solvation shell. Furthermore, methanol is attached with its polar hydroxyl group to the amide group so that its nonpolar methyl group is oriented toward the bulk solvent. This is in good agreement with findings of Pang et al.²⁰ who investigated the orientation of methanol and water at PNIPAAm monomers in water/methanol mixtures with molecular dynamics simulation in detail.

For the following discussion, it is assumed that the PNIPAAm chain together with its solvation shell can be considered as an entity, a standpoint that is supported by the strong H-bonding between the solvation shell and the chain and also by visualizations of the molecular trajectory. Due to the effect described above, the PNIPAAm chain + solvation shell has a hydrophobic methyl-rich surface. It is presumed that this leads to a solubility mismatch with water-rich bulk solvents and, consequently, the collapse of the hydrogel or the precipitation of the polymer in the region of cononsolvency. With increasing methanol mole fraction, the bulk solvent becomes more compatible with the hydrophobic PNIPAAm chain + solvation shell, leading to the disappearance of cononsolvency.

More detailed information on H-bonding statistics is given in Appendix B in the Supporting Information. This appendix also contains information on the visualization of the simulation results (Appendix C), some of which are made available in the Supporting Information of the present work.

CONCLUSION

The dependence of the volume transition of PNIPAAm hydrogels on the composition of the solvent in water/methanol mixtures was studied both by experiment and by molecular simulation. Cononsolvency was observed with both approaches. The region in which it occurs in the experimental studies of hydrogels is almost independent of the degree of cross-linking,

which indicates that the effect is related to the interactions between the hydrogel backbone polymer and the solvent.

Therefore, single polymer chains in explicit solvents were studied by molecular simulation. Force fields from the literature for the polymer chain, water, and methanol were selected that are capable to predict cononsolvency. The region in which it occurs is qualitatively and sometimes even quantitatively predicted by the simulations without adjusting any parameters.

The simulation results indicate that the reason for cononsolvency is the strong H-bonding between methanol and the PNIPAAm chain, which leads to a preferred molecular orientation of methanol, where the methyl group points toward the bulk solvent. The PNIPAAm chain + solvation shell entity therefore has a hydrophobic methyl-rich surface. This leads to a mismatch with water-rich bulk solvents and consequently to the collapse of the hydrogel or the precipitation of the polymer in the region of cononsolvency.

■ ASSOCIATED CONTENT

■ Supporting Information

In the Supporting Information, the Appendix and visualizations of the solvent structure around the PNIPAAm chains are contained. The Appendix contains the preliminary studies on the applicability of different methanol models for the investigations of the present work (Appendix A), a more detailed discussion of the H-bonds between the solvent and the PNIPAAm chain (Appendix B), and detailed information about the visualizations of the molecular simulations (Appendix C). The three visualizations show the structure and H-bonds of the solvents at different solvent compositions. The fourth visualization shows the local concentration of the solvents around the PNIPAAm chain in the cononsolvency region and the collapse of the chain. This material is available free of charge via the Internet at <http://pubs.acs.org>.

■ AUTHOR INFORMATION

Corresponding Author

*E-mail: hans.hasse@mv.uni-kl.de.

Notes

The authors declare no competing financial interest.

■ ACKNOWLEDGMENTS

We gratefully thank the German Research Foundation (DFG) for funding support within the Collaborative Research Centre 716. The computer simulations were carried out on the high-performance computer HP XC 4000 of the Steinbuch Centre for Computing in Karlsruhe (Germany) under the project LAMO. We also thank Thomaß Bertram, Sebastian Grottel, and Guido Reina from the Institute for Visualization and Interactive Systems at the University of Stuttgart (Germany) for their support with respect to visualization. The work was carried out under the auspices of the Boltzman-Zuse Society for Computational Molecular Engineering.

■ REFERENCES

- (1) El-Rehim, H. A. A. *Radiat. Phys. Chem.* **2005**, *74*, 111–117.
- (2) Pavlyuchenko, V. N.; Sorochinskaya, O. V.; Ivanchev, S. S.; Khaikin, S. Y.; Trounov, V. A.; Lebedev, V. T.; Sosnov, E. A.; Gofman, I. V. *Polym. Adv. Technol.* **2009**, *20*, 367–377.
- (3) Peppas, N.; Bures, P.; Leobandung, W.; Ichikawa, H. *Eur. J. Pharm. Biopharm.* **2000**, *50*, 27–46.
- (4) Slaughter, B. V.; Khurshid, S. S.; Fisher, O. Z.; Khademhosseini, A.; Peppas, N. A. *Adv. Mater.* **2009**, *21*, 3307–3329.
- (5) van der Linden, H.; Olthuis, W.; Bergveld, P. *Lab Chip* **2004**, *4*, 619–624.
- (6) Fujimoto, K. L.; Ma, Z.; Nelson, D. M.; Hashizume, R.; Guan, J.; Tobita, K.; Wagner, W. R. *Biomaterials* **2009**, *30*, 4357–4368.
- (7) Rzaev, Z. M. O.; Dinçer, S.; Piskin, E. *Prog. Polym. Sci.* **2007**, *32*, 534–595.
- (8) Hühner, A.; Schäfer, B.; Xu, X.; Maurer, G. *Phys. Chem. Chem. Phys.* **2002**, *4*, 835–844.
- (9) Hühner, A.; Maurer, G. *Fluid Phase Equilib.* **2004**, *226*, 321–332.
- (10) Hühner, A.; Xu, X.; Maurer, G. *Fluid Phase Equilib.* **2004**, *219*, 231–244.
- (11) Amiya, T.; Hirokawa, Y.; Hirose, Y.; Li, Y.; Tanaka, T. *J. Chem. Phys.* **1987**, *86*, 2375–2379.
- (12) Mukae, K.; Sakurai, M.; Sawamura, S.; Makino, K.; Kim, S. W.; Ueda, I.; Shirahama, K. *J. Phys. Chem.* **1993**, *97*, 737–741.
- (13) Crowther, H.; Vincent, B. *Colloid Polym. Sci.* **1998**, *276*, 46–51.
- (14) Althans, D.; Langenbach, K.; Enders, S. *Mol. Phys.* **2012**, DOI: 10.1080/00268976.2012.655339.
- (15) Schild, H. G.; Muthukumar, M.; Tirrell, D. A. *Macromolecules* **1991**, *24*, 948–952.
- (16) Tanaka, F.; Koga, T.; Winnik, F. M. *Phys. Rev. Lett.* **2008**, *101*, 028302.
- (17) Winnik, F. M.; Ringsdorf, H.; Venzmer, J. *Macromolecules* **1990**, *23*, 2415–2416.
- (18) Tanaka, F.; Koga, T.; Kojima, H.; Winnik, F. M. *Macromolecules* **2009**, *42*, 1321–1330.
- (19) Cheng, H.; Shen, L.; Wu, C. *Macromolecules* **2006**, *39*, 2325–2329.
- (20) Pang, J.; Yang, H.; Ma, J.; Cheng, R. *J. Phys. Chem. B* **2010**, *114*, 8652–8658.
- (21) Walter, J.; Ermatchkov, V.; Vrabec, J.; Hasse, H. *Fluid Phase Equilib.* **2010**, *296*, 164–172.
- (22) Jorgensen, W. L.; Tirado-Rives, J. *J. Am. Chem. Soc.* **1988**, *110*, 1657–1666.
- (23) Jorgensen, W. L.; Maxwell, D. S.; Tirado-Rives, J. *J. Am. Chem. Soc.* **1996**, *118*, 11225–11236.
- (24) Berendsen, H. J. C.; Grigera, J. R.; Straatsma, T. P. *J. Phys. Chem.* **1987**, *91*, 6269–6271.
- (25) Çaykara, T.; Kiper, S.; Demirel, G. *J. Appl. Polym. Sci.* **2006**, *101*, 1756–1762.
- (26) Heskins, M.; Guillet, J. E. *J. Macromol. Sci., Part A: Pure Appl. Chem.* **1968**, *8*, 1441–1455.
- (27) van Gunsteren, W. F.; Billeter, S.; Eising, A.; Hünenberger, P.; Krüger, P.; Mark, A.; Scott, W.; Tironi, I. *Biomolecular Simulation: The Gromos 96 Manual and User Guide*; vdf Hochschulverlag an der ETH Zürich: Zürich, Switzerland, 1996.
- (28) Schnabel, T.; Srivastava, A.; Vrabec, J.; Hasse, H. *J. Phys. Chem. B* **2007**, *111*, 9871–9878.
- (29) van der Spoel, D.; Lindahl, E.; Hess, B.; Kutzner, C.; van Buuren, A. R.; Apol, E.; Meulenhoff, P. J.; Tieleman, D. P.; Sijbers, A. L. T. M.; Feenstra, K. A.; van Drunen, R.; Berendsen, H. J. C. *Gromacs User Manual Version 4.0*; The GROMACS Development Team, 2006. www.gromacs.org.
- (30) van der Spoel, D.; Lindahl, E.; Hess, B.; Groenhof, G.; Mark, A. E.; Berendsen, H. J. C. *J. Comput. Chem.* **2005**, *26*, 1701–1718.
- (31) Hess, B.; Kutzner, C.; van der Spoel, D.; Lindahl, E. *J. Chem. Theory Comput.* **2008**, *4*, 435–447.
- (32) Berendsen, H. J. C.; Postma, J. P. M.; van Gunsteren, W. F.; DiNola, A.; Haak, J. R. *J. Chem. Phys.* **1984**, *81*, 3684–3690.
- (33) Bussi, G.; Donadio, D.; Parrinello, M. *J. Chem. Phys.* **2007**, *126*, 014101.
- (34) Hockney, R. W.; Goel, S. P.; Eastwood, J. W. *J. Comput. Phys.* **1974**, *14*, 148–158.
- (35) Essmann, U.; Perera, L.; Berkowitz, M. L.; Darden, T.; Lee, H.; Pedersen, L. G. *J. Chem. Phys.* **1995**, *103*, 8577–8592.
- (36) Haughney, M.; Ferrario, M.; McDonald, I. R. *J. Phys. Chem.* **1987**, *91*, 4934–4940.
- (37) Schnabel, T. Molecular modeling and simulation of hydrogen bonding pure fluids and mixtures. Ph.D. Thesis, Institut für

Technische Thermodynamik und Thermische Verfahrenstechnik, Universität Stuttgart, Stuttgart, Germany, 2008.

(38) Humphrey, W.; Dalke, A.; Schulten, K. *J. Mol. Graph.* **1996**, *14*, 33–38.

(39) Grottel, S.; Reina, G.; Dachsbacher, C.; Ertl, T. *Comput. Graph. Forum* **2010**, *29*, 953–962.

(40) Thomaß, B.; Walter, J.; Krone, M.; Hasse, H.; Ertl, T. *Interactive Exploration of Polymer-Solvent Interactions*; In International Workshop Vision, Modeling and Visualization, 2011; pp 301–308.

(41) Walter, J.; Deublein, S.; Vrabec, J.; Hasse, H. Development of Models for Large Molecules and Electrolytes in Solution for Process Engineering. In *High Performance Computing in Science and Engineering '09*; Nagel, W. E., Kröner, D. B., Resch, M. M., Eds.; Springer, Berlin: 2010; pp 165–176.